



HAL
open science

Background-Free Near-Infrared Biphoton Emission from Single GaAs Nanowires

Grégoire Saerens, Thomas Dursap, Ian Hesner, N. M. H. Duong, A. S. Solntsev, A. Morandi, A. Maeder, A. Karvounis, Philippe Regreny, R. J. Chapman, et al.

► To cite this version:

Grégoire Saerens, Thomas Dursap, Ian Hesner, N. M. H. Duong, A. S. Solntsev, et al.. Background-Free Near-Infrared Biphoton Emission from Single GaAs Nanowires. *Nano Letters*, 2023, 23 (8), pp.3245-3250. 10.1021/acs.nanolett.3c00026 . hal-04071266

HAL Id: hal-04071266

<https://hal.science/hal-04071266>

Submitted on 13 Oct 2023

HAL is a multi-disciplinary open access archive for the deposit and dissemination of scientific research documents, whether they are published or not. The documents may come from teaching and research institutions in France or abroad, or from public or private research centers.

L'archive ouverte pluridisciplinaire **HAL**, est destinée au dépôt et à la diffusion de documents scientifiques de niveau recherche, publiés ou non, émanant des établissements d'enseignement et de recherche français ou étrangers, des laboratoires publics ou privés.

1 Background-Free Near-Infrared Biphoton Emission
2 from Single GaAs Nanowires

3 *Grégoire Saerens^{a*}, Thomas Dursap^b, Ian Hesner^a, Ngoc M. H. Duong^a, Alexander S. Solntsev^c,*
4 *Andrea Morandi^a, Andreas Maeder^a, Artemios Karvounis^a, Philippe Regreny^b, Robert J.*
5 *Chapman^a, Alexandre Danescu^b, Nicolas Chauvin^b, José Penuelas^b and Rachel Grange^a*

6 ^a ETH Zurich, Department of Physics, Institute for Quantum Electronics, Optical Nanomaterial
7 Group, 8093 Zurich, Switzerland

8 ^b Univ. Lyon, CNRS, ECL, INSA Lyon, UCBL, CPE Lyon, INL, UMR 5270, 69130 Ecully,
9 France

10 ^c University of Technology Sydney, School of Mathematical and Physical Sciences, Ultimo,
11 New South Wales 2007, Australia

12

1 ABSTRACT:

2 The generation of photon pairs from nanoscale structures with high rates is still a challenge for the
3 integration of quantum devices as it suffers from parasitic signal from the substrate. In this work,
4 we report type-0 spontaneous parametric down-conversion at 1550 nm from individual bottom-up
5 grown zinc-blende GaAs nanowires with lengths of up to 5 μm and diameters of up to 450 nm.
6 The Nanowires were deposited on a transparent ITO substrate and we measured a background-free
7 coincidence rate of 0.05 Hz in a Hanbury-Brown-Twiss setup. Taking into account transmission
8 losses, the pump fluence and the nanowire volume, we achieved a biphoton generation of 60
9 GHz/Wm, which is at least 3 times higher than in previously reported single nonlinear micro- and
10 nanostructures. We also studied the correlations between the second-harmonic generation and the
11 spontaneous parametric down-conversion intensities with respect to the pump polarization and in
12 different individual nanowires.

13 KEYWORDS Spontaneous parametric down-conversion, second-harmonic generation, III-V
14 semiconductors, GaAs nanowires, room temperature.

15

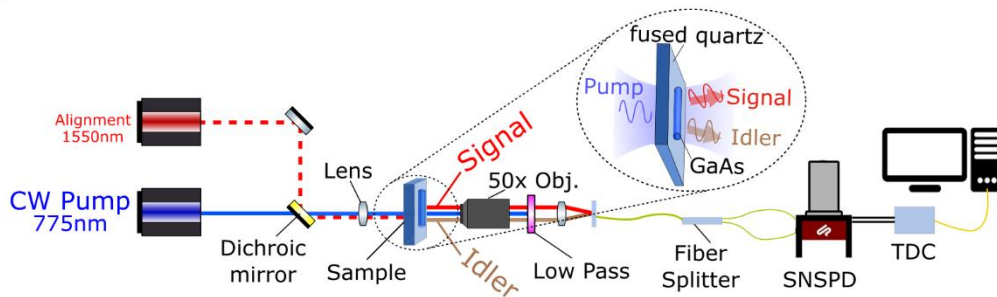
1 Miniaturization of biphoton light sources is an important requirement to achieve scalable and
2 stable integrated quantum devices.¹ Photon pairs, or similarly heralded single photons, generated
3 via spontaneous parametric down-conversion (SPDC) profit from high indistinguishability, room-
4 temperature operation, simple signal filtering, coherent emission as well as entanglement in several
5 degrees of freedom.²⁻⁴ Applications have been demonstrated in different quantum technologies,
6 including communication,⁵⁻¹⁰ imaging,¹¹⁻¹³ computing¹⁴⁻¹⁶ and metrology.¹⁷⁻¹⁹ Despite its
7 intrinsically limited efficiency to avoid multi-photon events, compared, for example, to quantum
8 dot- or atom-based photon sources,^{20,21} the brightness of SPDC-based photon sources can be
9 improved with multiplexing without an increase in unwanted double photon pairs.^{1,22,23}

10 Today's leading nonlinear light sources are bulk birefringent or periodically-poled crystals,²⁴⁻²⁶
11 and periodically poled waveguides,²⁷⁻³⁰ with millimeter length scales, for which phase matching
12 is required. Miniaturization to the micron or sub-micron scale, to sizes smaller than the coherence
13 length, relaxes the phase-matching condition and reduces the footprint of the source.³¹ SPDC with
14 no phase matching requirements has recently been demonstrated in thin films,³²⁻³⁴ and
15 metasurfaces,³⁵⁻³⁸ for example by taking advantage of resonances such as bound states in the
16 continuum or Mie resonances. A single nanoantenna does not need phase matching either,³⁹ and
17 arrays of nanoantenna can be collectively excited for increased generation rate. To our knowledge,
18 SPDC generation from a single structure has only been demonstrated at 1550 nm in two different
19 types of geometries, top-down AlGaAs nanoresonators⁴⁰ and free-standing LiNbO₃ microcubes.⁴¹
20 This has however not been demonstrated in GaAs nanostructures despite the strong $\chi^{(2)}$ tensor
21 ($d_{36}=370$ pm/V⁴²), high refractive index (3.4 for λ around 1550nm⁴³) and various fabrication
22 methods.

1 Here we report type-0 SPDC in individual self-assisted grown zinc-blende (ZB) GaAs nanowires
2 (NWs) with lengths of $5.2 \pm 0.4 \mu\text{m}$ and diameter of $430 \pm 30 \text{ nm}$. Due to the high tensor
3 components of the GaAs crystal structure compared to other typical nonlinear materials (β -barium
4 borate, potassium dihydrogen phosphate or lithium niobate), and the possibility to place the
5 structure on a transparent substrate, we obtained at room temperature and for 15 mW incident
6 power a high photon-pair rate of 0.05Hz with a corresponding coincidences-to-accidentals ratio
7 (CAR) of 60 in the coincidence histogram. The efficiency given as a transmission-corrected photon
8 pair rate normalized to the excitation fluence and nanostructure volume was 60 GHz/Wm. This is
9 40 times higher than AlGaAs nanoresonator⁴⁰ and 3 times higher than LiNbO₃ microcube
10 systems.⁴¹

11 Self-assisted GaAs NWs with ZB crystal structure and a slight Be p-doping were grown by
12 molecular beam epitaxy on a silicon (111) substrate. It should be noted that the NWs possess also
13 a short defective region at the bottom and at the top, including a wurtzite (WZ) segment at the
14 top.⁴⁴ We will discuss this aspect again in the experimental section. After growth, the NWs were
15 mechanically transferred to a transparent thin ITO layer (10nm) on SiO₂ substrate. The detailed
16 fabrication steps are given in section 1 of the Supporting Information. In section 2 of the
17 Supporting Information, we characterized the NWs optically. We show on the one hand that the
18 NWs are non-resonant around 775 nm by collecting the scattering spectrum using a dark field
19 microscope. On the other hand, we confirm optically the crystal uniformity in the middle of the
20 NWs by imaging the dependence of the second-harmonic generation (SHG) intensity with the
21 linear polarization of the incoming pump laser.⁴⁵ We recorded SPDC with a Hanbury-Brown-
22 Twiss (HBT) setup as shown in Figure 1. Firstly, a linearly polarized continuous-wave laser with
23 a wavelength of 775 nm and 15 mW power was focused with a lens ($f = 8 \text{ mm}$) on a single NW.

1 The generated photon pairs were then collected with a 50x NIR objective ($f = 4 \text{ mm}$) and separated
 2 from the pump with two low-pass filters. After that, the light was coupled to a 1550 nm fiber, split
 3 in two channels and finally detected with superconducting nanowire single-photon detectors
 4 (SNSPDs). A time-to-digital converter (TDC) was used to measure coincidence counts between
 5 the two channels. A second 1550 nm laser was used for the SHG process and to maximize the fiber
 6 transmission and detection efficiency. In section 3 of the Supporting Information, we describe in
 7 detail the setup and give the alignment procedure to measure photon pairs. Additionally, we
 8 discuss in section 4 of the Supporting Information, the impact of the pump wavelength, which is
 9 smaller than the bandgap of GaAs.

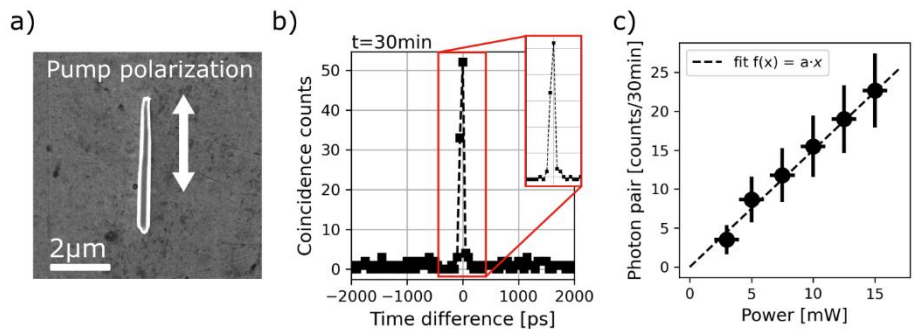


10

11 **Figure 1.** Hanbury-Brown-Twiss (HBT) setup using a continuous-wave pump laser with
 12 wavelength at 775nm. The photon pairs are collected with a 50x objective and filtered with two
 13 low-pass filters. Photons are detected with superconducting nanowire single-photon detectors
 14 (SNSPDs) and the coincidence counts of two channels are measured using a time-to-digital
 15 converter (TDC). The transmission in the fiber and the detection efficiency are both maximized
 16 using a 1550 nm laser.

17 We excite a GaAs NW with a length of $5 \mu\text{m}$ and a diameter of 450 nm using a linearly polarized
 18 laser along its crystal axis, with a spot size of around $6 \mu\text{m}$ radius (Figure 2a). The measured
 19 coincidence counts over 30 min show a photon pair rate of 0.05Hz (90 counts over 30 min, see

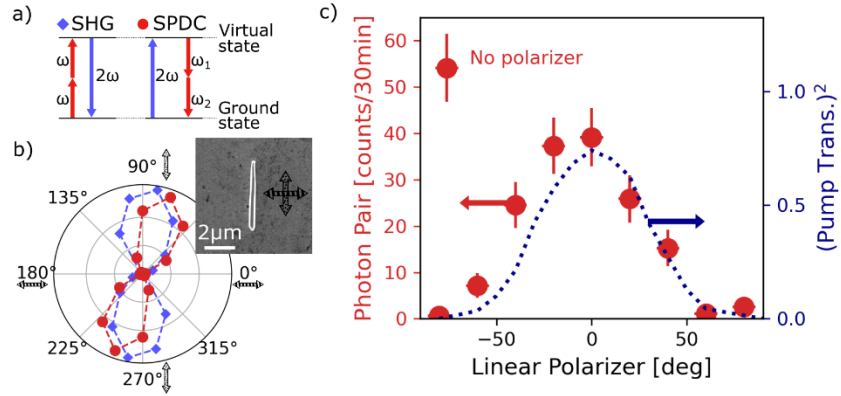
1 Figure 2b) with a CAR equal to 60, which should be greater than 2 for photon pairs. The SPDC
 2 process is also confirmed by the linear increase in photon-pairs with respect to the incoming power,
 3 as shown in Figure 2c, indicating that only one photon is involved as pump in the nonlinear
 4 process. Phase matching in such nanostructures is not necessary as the coherence length of GaAs
 5 is around $2.7 \mu\text{m}$, which is much more than the thickness of the NW (see calculation in section 4
 6 of the Supporting Information).



7
 8 **Figure 2.** a) Scanning electron microscopy image (SEM) of the GaAs nanowire (NW) with a
 9 length of $5 \mu\text{m}$ and a diameter of 450 nm. The linear polarization of the pump, which is along the
 10 long axis of the NW, is indicated by the white arrow. b) Coincidence counts measured over 30 min
 11 with a maximum count of 52 at zero-time difference and a coincidences-to-accidentals ratio (CAR)
 12 well above 2. The detected biphoton arrivals is calculated as the sum of the coincidence counts
 13 around zero-time difference, which is here 90. c) Linear dependence of photon pair counts with
 14 incoming pump power.

15 From the quantum-classical correspondence relation between SPDC and SHG as depicted in
 16 Figure 3a,⁴⁶ we expected a similar polarization dependency of the second-order nonlinear signals
 17 for non-resonant structures⁴¹ and we could indeed observe it. The SPDC (SHG) intensity measured
 18 for different polarizations of the 775 nm (1550nm) pump laser is indicated by red circles (blue
 19 diamonds) in Figure 3b. A maximum SPDC (SHG) signal intensity was obtained for a linear

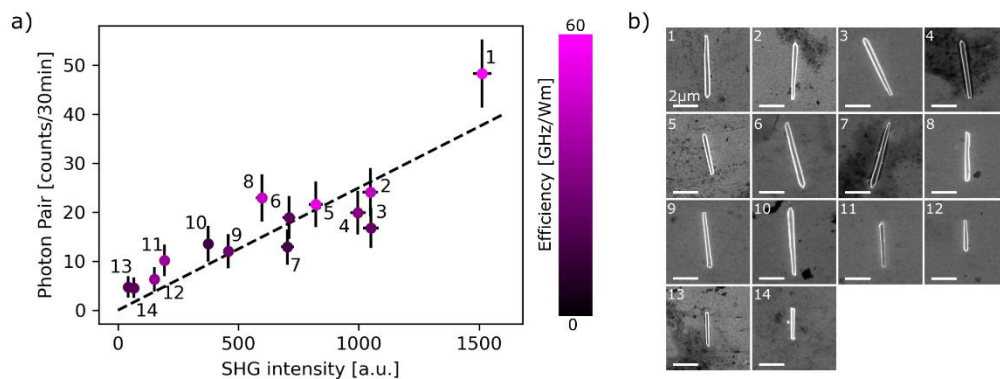
1 polarization along the NW. In addition, we characterized the polarization of the photon pairs by
2 placing a linear polarizer before the fiber coupling. The linear polarization of the pump was fixed
3 along the NW, for which the photon-pair rate without polarizer was the highest, as shown
4 previously in Figure 2b. Figure 3c shows in red the photon pair counts without polarizer and for
5 different orientations of the polarizer. We measured a maximum photon-pair rate for the polarizer
6 oriented along the NW and no signal for the polarizer oriented perpendicularly to the NW. As a
7 matter of fact, the maximum rate was only $(90\%)^2$ that of the biphoton rate without polarizer,
8 which corresponds to the transmission losses of photon pairs from the polarizer. We compared the
9 impact of the polarizer's rotation on the photon-pair rate (red points) directly with the transmission
10 squared of a 1550 nm laser (blue curve), for which the linear polarization was the same as the
11 SPDC pump laser. We observed a very good matching, as shown in Figure 3c. We thus conclude
12 that the SPDC is type-0 for NWs pumped along the long axis. Polarization-dependent Raman
13 scattering, SHG or single photon emission were already observed from single NWs.^{45,47–50}
14 Considering the crystal structure orientation of GaAs, in our case, the dependency of SHG and
15 SPDC on the pump polarization matches the expectation from our calculation of the $\chi^{(2)}$ tensor in
16 the new rotation frame. In section 5 of the Supporting Information we show similar polarization-
17 dependent SHG emission profiles for 14 different structures. The second-order nonlinear emission
18 from GaAs, described in bulk by the strong d_{36} component, should in this case indeed lead to a
19 strong SHG emission intensity for a polarization along the x-axis, which is along the NW's axis.
20 The slight mismatch between the polarization measurement shown in Figure. 3b and 3c can be
21 understood from the alignment procedure, which involves multiple waveplates (see section 3 in
22 the Supporting Information).



1
2 **Figure 3.** a) Schematic of energy transitions involved in the SHG and SPDC process. b)
3 Normalized SHG (blue diamond) and SPDC (red circle) signal for different linear polarization
4 orientations of the pump. The inset shows the same SEM image of the NW as Figure 2a. The
5 lighter (darker) arrow corresponds to pump photons linearly polarized at 90°/270° (0°/180°) with
6 respect to the horizon (laboratory reference frame). c) Similar measurement at a fixed pump
7 polarization (90°/270°) with a linear polarizer set before the fiber in-coupling. We give with red
8 dots, the photon-pairs measured for different orientations of the polarizer and with the blue dotted
9 line the expected squared transmission from photons polarized along the NW's axis, as the 775
10 nm pump laser.

11 Finally, we measured similarly the second-order nonlinear intensities (SHG and SPDC) from 14
12 single GaAs NWs. We observed a linear correlation between SHG intensity and biphoton rates, as
13 shown in Figure 4. NWs generating low SHG intensities also emit low photon-pair rates. We
14 noticed that the nonlinear emission intensity was not depending on the NW's size, see for example
15 NW n° 10 in Figure 4 with a higher volume compared to the average but with lower nonlinear
16 intensities. We confirm this dependency by analyzing more in detail the impact of the NW's size
17 on the biphoton rate (see section 6 of the Supporting Information). We also evaluated for each NW
18 if their linear optical properties are correlated with the nonlinear properties. When taking into

1 account the losses in the setup (objective transmission, fiber in-coupling, fiber splitter and
 2 detector), we find a photon pair rate of up to 20Hz. This correction does not take into account
 3 photon pairs emitted backwards or forward but only collected by a NA=0.65 objective. In order to
 4 compare with other miniaturized sources, we normalized this transmission corrected rate as in
 5 Marino et al.⁴⁰ with the volume of the NW and the pump fluence. The resulting efficiency of the
 6 SPDC process can reach 60 GHz/Wm for GaAs NWs (see purple scale bar in Figure 4a). The
 7 detailed calculations, the numerical values of the efficiencies are given in section 6 of the
 8 Supporting Information. The overall crystal structure uniformity is shown in Figures S3 and S4 of
 9 the Supporting Information, but nanoscopic crystal structure defects or doping concentration
 10 variations may be present and could still have some impact on the biphoton emission efficiency.



11
 12 **Figure 4.** a) Correlation between SHG (x-axis) and SPDC (y-axis) intensity for 14 different NWs.
 13 The measured biphoton rates normalized to the transmission losses, volume and (fixed) pump
 14 fluence are given as efficiencies with the pink scale bar. The maximum calculated efficiency was
 15 60 GHz/Wm. b) SEM images of the 14 single NWs.

16 In comparison, the SPDC efficiency from GaAs NWs is 40 times higher in similar AlGaAs
 17 nanoantennas⁴⁰ and 3 times higher than in LiNbO₃ microcubes.⁴¹ We consider this was possible
 18 thanks to the NW's growth and transfer method and the geometry of the system, the one-

1 dimensionality of the NW, leading to an accessible and strong d_{36} component of the bulk GaAs ZB
2 $\chi^{(2)}$ tensor.

3

4 CONCLUSION:

5 We have investigated type 0 photon pairs generated at 1550 nm wavelength from SPDC in single
6 GaAs NWs. We have tested the quantum-classical correspondence by comparing on the one hand
7 the pump polarization impact on the SHG intensity with the SPDC rate, and on the other hand the
8 nonlinear generation from 14 similar NWs. We observed a linear correlation between SPDC and
9 SHG intensities. For individual self-assisted grown ZB GaAs NW with 5 μm length and 450 nm
10 diameter we obtained a maximum photon pair rate of 20 Hz. We have demonstrated GaAs NWs
11 as photon pair sources profiting from stability, time coherence and room temperature operation.
12 These structures could be directly grown on a photonic chip or transferred and freely positioned
13 on it using an atomic force microscopy tip. They would act as quantum light emitters that do not
14 need quantum confinement engineering. Further study into the geometry and crystal orientation of
15 III-V nanostructures would benefit not only research in nonlinear processes such as SHG and
16 SPDC, but also in single photon emitters such as defects and quantum dots.

17

18 ASSOCIATED CONTENT

19 **Supporting Information.** Details about fabrication, nanowires optical characterization, setup
20 and alignment to measure SHG and SPDC, the GaAs coherence length, the GaAs bulk $\chi^{(2)}$
21 tensor specific to this experiment and the summary of the NWs efficiency are available as
22 Supporting Information. The following file is available free of charge
23 (“Supplementary_Material.docx”).

1 AUTHOR INFORMATION

2 **Corresponding Author**

3 * gsaerens@phys.ethz.ch

4 **Author Contributions**

5 The manuscript was written through contributions of all authors. R.G., R.J.C., A.S.S. and G.S.
6 designed the experiment. G.S., A.Mae. and N.D. built the setup and G.S. and I.H. conducted the
7 experiments. T.D., P.R., A.D., N.C. and J.P. fabricated the GaAs NWs and did the
8 photoluminescence measurements. A.Mo. and A.K. took the SEM images of the NWs. G.S., T.D.,
9 R.J.C. and R.G. wrote the manuscript. All authors have given approval to the final version of the
10 manuscript

11 **Funding Sources**

12 The European Research Council (714837), the Australian Research Council (DE180100070) and
13 the French Agence Nationale de la Recherche (ANR) (BEEP ANR-18-CE05-0017-01).

14 **Notes**

15 ACKNOWLEDGMENT

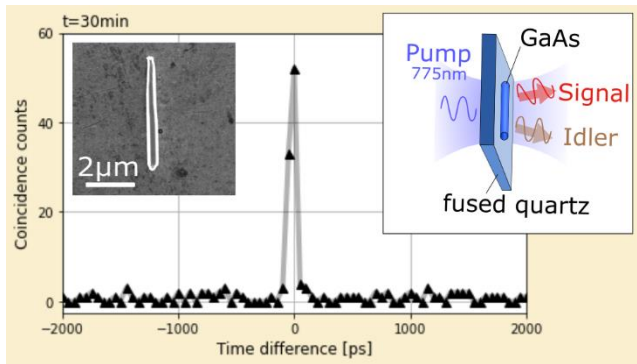
16 The authors thank the Scientific Centre for Optical and Electron Microscopy (ScopeM) of
17 Eidgenössische Technische Hochschule (ETH) Zürich and the NanoLyon platform for the access
18 to the equipments and J. B. Goure for technical assistance. This work was supported by the
19 European Union's Horizon 2020 research and innovation program from the European Research
20 Council under the Grant Agreement No. 714837 (Chi2-nano-oxides), the Australian Research

1 Council DE180100070 and the French Agence Nationale de la Recherche (ANR) for funding
2 (project BEEP ANR-18-CE05-0017-01).

3 ABBREVIATIONS

4 NW nanowire, SPDC spontaneous parametric down-conversion, SHG second-harmonic
5 generation, ZB zinc-blende, CAR coincidences-to-accidentals, HBT Hanbury-Brown-Twiss,
6 SNSPD superconducting nanowire single-photon detector, TDC time-to-digital converter.

7 TOC



8

9

1 REFERENCES

- 2 (1) Meyer-Scott, E.; Silberhorn, C.; Migdall, A. Single-Photon Sources: Approaching the Ideal
3 through Multiplexing. *Rev. Sci. Instrum.* **2020**, *91* (4), 041101.
- 4 (2) Meraner, S.; Chapman, R. J.; Frick, S.; Prilmüller, M.; Weihs, G. Approaching the Tsirelson
5 Bound with a Sagnac Source of Polarization-Entangled Photons. *SciPost Phys.* **2021**, *10*
6 (017), 1–18.
- 7 (3) Brendel, J.; Gisin, N.; Tittel, W.; Zbinden, H. Pulsed Energy-Time Entangled Twin-Photon
8 Source for Quantum Communication. *Phys. Rev. Lett.* **1999**, *82* (12), 2594.
- 9 (4) Morrison, C. L.; Graffitti, F.; Barrow, P.; Pickston, A.; Ho, J.; Fedrizzi, A. Frequency-Bin
10 Entanglement from Domain-Engineered down-Conversion. *APL Photonics* **2022**, *7* (6),
11 066102.
- 12 (5) Burnham, D. C.; Weinberg, D. L. Observation of Simultaneity in Parametric Production of
13 Optical Photon Pairs. *Phys. Rev. Lett.* **1970**, *25* (2), 84–87.
- 14 (6) Bouwmeester, D.; Pan, J. W.; Mattle, K.; Eibl, M.; Weinfurter, H.; Zeilinger, A.
15 Experimental Quantum Teleportation. *Nature* **1997**, *390*, 575–579.
- 16 (7) Jennewein, T.; Simon, C.; Weihs, G.; Weinfurter, H.; Zeilinger, A. Quantum Cryptography
17 with Entangled Photons. *Phys. Rev. Lett.* **2000**, *84* (20), 4.
- 18 (8) Ursin, R.; Tiefenbacher, F.; Schmitt-Manderbach, T.; Weier, H.; Scheidl, T.; Lindenthal,
19 M.; Blauensteiner, B.; Jennewein, T.; Perdigues, J.; Trojek, P.; et al. Entanglement-Based
20 Quantum Communication over 144km. *Nat. Phys.* **2007**, *3* (7), 481–486.
- 21 (9) Lo, H. K.; Curty, M.; Tamaki, K. Secure Quantum Key Distribution. *Nat. Photonics* **2014**,

- 1 8 (8), 595–604.
- 2 (10) Wang, X. L.; Cai, X. D.; Su, Z. E.; Chen, M. C.; Wu, D.; Li, L.; Liu, N. Le; Lu, C. Y.; Pan,
3 J. W. Quantum Teleportation of Multiple Degrees of Freedom of a Single Photon. *Nature*
4 **2015**, *518* (7540), 516–519.
- 5 (11) Pittman, T. B.; Shih, Y. H.; Strekalov, D. V.; Sergienko, A. V. Optical Imaging by Means
6 of Two-Photon Quantum Entanglement. *Phys. Rev. A* **1995**, *52* (5), 3429.
- 7 (12) Wolley, O.; Gregory, T.; Beer, S.; Higuchi, T.; Padgett, M. Quantum Imaging with a Photon
8 Counting Camera. *Sci. Rep.* **2022**, *12* (1), 1–9.
- 9 (13) Lugiato, L. A.; Gatti, A.; Brambilla E. Quantum Imaging. *J. Opt. B Quantum Semiclass.*
10 *Opt.* **2002**, *4*, S176–S183.
- 11 (14) Pittman, T. B.; Fitch, M. J.; Jacobs, B. C.; Franson, J. D. Experimental Controlled-NOT
12 Logic Gate for Single Photons in the Coincidence Basis. *Phys. Rev. A - At. Mol. Opt. Phys.*
13 **2003**, *68* (3), 4, 032316.
- 14 (15) Zhong, H. Sen; Li, Y.; Li, W.; Peng, L. C.; Su, Z. E.; Hu, Y.; He, Y. M.; Ding, X.; Zhang,
15 W.; Li, H.; et al. 12-Photon Entanglement and Scalable Scattershot Boson Sampling with
16 Optimal Entangled-Photon Pairs from Parametric Down-Conversion. *Phys. Rev. Lett.* **2018**,
17 *121* (25), 1–6.
- 18 (16) Heitert, P.; Buldt, F.; Bassène, P.; N’Gom, M. Producing Multiple Qubits via Spontaneous
19 Parametric Down-Conversion. *Phys. Rev. Appl.* **2021**, *16* (6), 1, 064048.
- 20 (17) Brida, G.; Genovese, M.; Gramegna, M.; Rastello, M. L.; Chekhova, M.; Krivitsky, L.
21 Single-Photon Detector Calibration by Means of Conditional Polarization Rotation. *J. Opt.*

- 1 *Soc. Am. B* **2005**, 22 (2), 488.
- 2 (18) Castelletto, S.; Degiovanni, I. P.; Schettini, V.; Migdall, A. Optimizing Single-Photon-
3 Source Heralding Efficiency and Detection Efficiency Metrology at 1550 Nm Using
4 Periodically Poled Lithium Niobate. *Metrologia* **2006**, 43 (2), 56-60.
- 5 (19) Polino, E.; Valeri, M.; Spagnolo, N.; Sciarrino, F. Photonic Quantum Metrology. *AVS*
6 *Quantum Sci.* **2020**, 2 (2), 024703.
- 7 (20) Somaschi, N.; Giesz, V.; De Santis, L.; Loredò, J. C.; Almeida, M. P.; Hornecker, G.;
8 Portalupi, S. L.; Grange, T.; Antón, C.; Demory, J.; et al. Near-Optimal Single-Photon
9 Sources in the Solid State. *Nat. Photonics* **2016**, 10 (5), 340–345.
- 10 (21) Jöns, K. D.; Schweickert, L.; Versteegh, M. A. M.; Dalacu, D.; Poole, P. J.; Gulinatti, A.;
11 Giudice, A.; Zwiller, V.; Reimer, M. E. Bright Nanoscale Source of Deterministic
12 Entangled Photon Pairs Violating Bell’s Inequality. *Sci. Rep.* **2017**, 7 (1), 1–11.
- 13 (22) Collins, M. J.; Xiong, C.; Rey, I. H.; Vo, T. D.; He, J.; Shahnia, S.; Reardon, C.; Krauss, T.
14 F.; Steel, M. J.; Clark, A. S.; et al. Integrated Spatial Multiplexing of Heralded Single-
15 Photon Sources. *Nat. Commun.* **2013**, 4 (May), 1–7.
- 16 (23) Mower, J.; Englund, D. Efficient Generation of Single and Entangled Photons on a Silicon
17 Photonic Integrated Chip. *Phys. Rev. A - At. Mol. Opt. Phys.* **2011**, 84 (5), 1–7.
- 18 (24) Li, L.; Liu, Z.; Ren, X.; Wang, S.; Su, V. C.; Chen, M. K.; Chu, C. H.; Kuo, H. Y.; Liu, B.;
19 Zang, W.; et al. Metalens-Array-Based High-Dimensional and Multiphoton Quantum
20 Source. *Science (80-.)*. **2020**, 368 (6498), 1487–1490.
- 21 (25) Kwiat, P. G.; Mattle, K.; Weinfurter, H.; Zeilinger, A.; Sergienko, A. V.; Shih, Y. New

- 1 High-Intensity Source of Polarization-Entangled Photon Pairs. *Phys. Rev. Lett.* **1995**, 75
2 (24), 4337–4341.
- 3 (26) Mair, A.; Vaziri, A.; Weihs, G.; Zeilinger, A. Entanglement of the Orbital Angular
4 Momentum States of Photons. *Nature* **2001**, 412, 313–316.
- 5 (27) Kurimura, S.; Kato, Y.; Maruyama, M.; Usui, Y.; Nakajima, H. Quasi-Phase-Matched
6 Adhered Ridge Waveguide in LiNb O₃. *Appl. Phys. Lett.* **2006**, 89 (19), 191123.
- 7 (28) Xue, G. T.; Niu, Y. F.; Liu, X.; Duan, J. C.; Chen, W.; Pan, Y.; Jia, K.; Wang, X.; Liu, H.
8 Y.; Zhang, Y.; et al. Ultrabright Multiplexed Energy-Time-Entangled Photon Generation
9 from Lithium Niobate on Insulator Chip. *Phys. Rev. Appl.* **2021**, 15 (6), 1.
- 10 (29) Zhao, J.; Ma, C.; Rüsing, M.; Mookherjea, S. High Quality Entangled Photon Pair
11 Generation in Periodically Poled Thin-Film Lithium Niobate Waveguides. *Phys. Rev. Lett.*
12 **2020**, 124 (16), 163603.
- 13 (30) Briggs, I.; Hou, S.; Cui, C.; Fan, L. Simultaneous Type-I and Type-II Phase Matching for
14 Second-Order Nonlinearity in Integrated Lithium Niobate Waveguide. *Opt. Express* **2021**,
15 29 (16), 26183.
- 16 (31) Saleh, H. D.; Vezzoli, S.; Caspani, L.; Branny, A.; Kumar, S.; Gerardot, B. D.; Faccio, D.
17 Towards Spontaneous Parametric down Conversion from Monolayer MoS₂. *Sci. Rep.* **2018**,
18 8 (1), 1–7.
- 19 (32) Okoth, C.; Cavanna, A.; Santiago-Cruz, T.; Chekhova, M. V. Microscale Generation of
20 Entangled Photons without Momentum Conservation. *Phys. Rev. Lett.* **2019**, 123 (26),
21 263602.

- 1 (33) Sultanov, V.; Santiago-Cruz, T.; Chekhova, M. V. Flat-Optics Generation of Broadband
2 Photon Pairs with Tunable Polarization Entanglement. *Opt. Lett.* **2022**, *47* (15), 3872.
- 3 (34) Guo, Q.; Qi, X.-Z.; Gao, M.; Hu, S.; Zhang, L.; Zhou, W.; Zang, W.; Zhao, X.; Wang, J.;
4 Yan, B.; et al. Ultrathin Quantum Light Source Enabled by a Nonlinear van Der Waals
5 Crystal with Vanishing Interlayer-Electronic-Coupling. **2022**, 1–15.
- 6 (35) Santiago-Cruz, T.; Fedotova, A.; Sultanov, V.; Weissflog, M. A.; Arslan, D.; Younesi, M.;
7 Pertsch, T.; Staude, I.; Setzpfandt, F.; Chekhova, M. Photon Pairs from Resonant
8 Metasurfaces. *Nano Lett.* **2021**, *21* (10), 4423–4429.
- 9 (36) Parry, M.; Mazzanti, A.; Poddubny, A.; Valle, G. Della; Neshev, D. N.; Sukhorukov, A. A.
10 Enhanced Generation of Nondegenerate Photon Pairs in Nonlinear Metasurfaces. *Adv.*
11 *Photonics* **2021**, *3* (5), 1–6.
- 12 (37) Zhang, J.; Ma, J.; Parry, M.; Cai, M.; Camacho-Morales, R.; Xu, L.; Neshev, D. N.;
13 Sukhorukov, A. A. Spatially Entangled Photon Pairs from Lithium Niobate Nonlocal
14 Metasurfaces. *Sci. Adv.* **2022**, *8* (30), 1–20.
- 15 (38) Poddubny, A. N.; Neshev, D. N.; Sukhorukov, A. A. Quantum Nonlinear Metasurfaces. In
16 *Nonlinear Meta-Optics*; CRC Press, Ed.; 2020; pp 147–180.
- 17 (39) Nikolaeva, A.; Frizyuk, K.; Olekhno, N.; Solntsev, A.; Petrov, M. Directional Emission of
18 Down-Converted Photons from a Dielectric Nanoresonator. *Phys. Rev. A* **2021**, *103* (4),
19 43703.
- 20 (40) Marino, G.; Solntsev, A. S.; Xu, L.; Gili, V. F.; Carletti, L.; Poddubny, A. N.; Rahmani, M.;
21 Smirnova, D. A.; Chen, H.; Lemaître, A.; et al. Spontaneous Photon-Pair Generation from

- 1 a Dielectric Nanoantenna. *Optica* **2019**, *6* (11), 1416.
- 2 (41) Duong, N. M. H.; Saerens, G.; Timpu, F.; Buscaglia, M. T.; Buscaglia, V.; Morandi, A.;
3 Muller, J. S.; Maeder, A.; Kaufmann, F.; Solntsev, A. S.; et al. Spontaneous Parametric
4 Down-Conversion in Bottom-up Grown Lithium Niobate Microcubes. *Opt. InfoBase Conf.*
5 *Pap.* **2022**, *12* (9), 3696–3704.
- 6 (42) Boyd, R. W. *Nonlinear Optics*; Elsevier Science Publishing Co Inc, 2008, pp 1-67.
- 7 (43) Papatryfonos, K.; Angelova, T.; Brimont, A.; Reid, B.; Guldin, S.; Smith, P. R.; Tang, M.;
8 Li, K.; Seeds, A. J.; Liu, H.; et al. Refractive Indices of MBE-Grown Al_xGa(1-x)As
9 Ternary Alloys in the Transparent Wavelength Region. *AIP Adv.* **2021**, *11* (2), 025327.
- 10 (44) Dursap, T.; Vettori, M.; Danescu, A.; Botella, C.; Regreny, P.; Patriarche, G.; Gendry, M.;
11 Penuelas, J. Crystal Phase Engineering of Self-Catalyzed GaAs Nanowires Using a RHEED
12 Diagram. *Nanoscale Adv.* **2020**, *2* (5), 2127–2134.
- 13 (45) Timofeeva, M.; Bouravleuv, A.; Cirlin, G.; Shtrom, I.; Soshnikov, I.; Reig Escalé, M.;
14 Sergeyev, A.; Grange, R. Polar Second-Harmonic Imaging to Resolve Pure and Mixed
15 Crystal Phases along GaAs Nanowires. *Nano Lett.* **2016**, *16* (10), 6290–6297.
- 16 (46) Lenzini, F.; Poddubny, A. N.; Titchener, J.; Fisher, P.; Boes, A.; Kasture, S.; Haylock, B.;
17 Villa, M.; Mitchell, A.; Solntsev, A. S.; et al. Direct Characterization of a Nonlinear
18 Photonic Circuit's Wave Function with Laser Light. *Light Sci. Appl.* **2018**, *7* (1), 17143–
19 17145.
- 20 (47) Xiong, Q.; Chen, G.; Gutierrez, H. R.; Eklund, P. C. Raman Scattering Studies of Individual
21 Polar Semiconducting Nanowires: Phonon Splitting and Antenna Effects. *Appl. Phys. A*

- 1 *Mater. Sci. Process.* **2006**, 85 (3), 299–305.
- 2 (48) Ren, M. L.; Liu, W.; Aspetti, C. O.; Sun, L.; Agarwal, R. Enhanced Second-Harmonic
3 Generation from Metal-Integrated Semiconductor Nanowires via Highly Confined
4 Whispering Gallery Modes. *Nat. Commun.* **2014**, 5, 5432.
- 5 (49) de Ceglia, D.; Carletti, L.; Galtarossa, A.; Vincenti, M. A.; de Angelis, C.; Scalora, M.
6 Harmonic Generation in Mie-Resonant GaAs Nanowires. *Appl. Sci.* **2019**, ~~9Part F143~~,
7 3381.
- 8 (50) Yu, P.; Li, Z.; Wu, T.; Wang, Y. T.; Tong, X.; Li, C. F.; Wang, Z.; Wei, S. H.; Zhang, Y.;
9 Liu, H.; et al. Nanowire Quantum Dot Surface Engineering for High Temperature Single
10 Photon Emission. *ACS Nano* **2019**, 13 (11), 13492–13500.

11